Advanced Materials '93, I / B: Magnetic, Fullerene, Dielectric, Ferroelectric,
Diamond and Related Materials, edited by M. Homma et al.
Trans. Mat. Res. Soc. Jpn., Volume 14B

Magnetic properties and microstructure of Fe_3B-based Nd-Fe-B hard magnetic materials

Satoshi Hirosawa and Hirokazu Kanekiyo

Research and Development Division, Sumitomo Special Metals Company, Limited
2-15-17 Egawa, Shimamoto-cho, Osaka 618, Japan

Effects of additive elements on microstructure and magnetic properties of nanocrystalline Nd-Fe-B hard magnetic materials consisting of soft magnetic Fe_3B and hard magnetic $Nd_2Fe_{14}B$ are described. The magnets are isotropic, and are produced near the composition of $Nd_{4.5}Fe_{77}B_{18.5}$ by heating amorphous materials obtained by melt-spinning, whereby the metastable nanostructure appears. Effects of simultaneous addition of V or Co with M, where M is Si or Ga, are extensively studied. The Co-M and V-Si additions effectively enhance remanence B_r, the maximum energy product $(BH)_{max}$, and the intrinsic coercivity H_{cJ}. Partial substitution of Nd with Dy give an additional increase in H_{cJ}. Compression-molded, resin-bonded magnets exhibit magnetic performances in the following range; H_{cJ} = 310-470 kA/m, B_r = 0.7-0.9 T, and $(BH)_{max}$ = 50-73 kJ/m^3. The magnets can be magnetized to the 95% saturation with magnetizing forces as small as 1 MA/m and have excellent thermal stability, and hence, may be utilized in applications such as high-precision small motors.

1. INTRODUCTION

Fe_3B-based hard magnetic materials were first discovered by Coehoorn *et al.*[1,2] and drew attention because of a high remanence values (B_r). However, the intrinsic coercivities (H_{cJ}) were not large enough for a practical usage. This magnet is composed of Fe_3B, $Nd_2Fe_{14}B$, and bcc Fe. Early efforts to improve the materials include: optimization of composition of the ternary magnets[3-7], partial substitution of Nd with Tb or Dy[8,9], and partial substitution of Fe by Co[10] or Ni[11]. Sizable increase in H_{cJ} was observed only in the case of Tb/Dy substitution for Nd, where a significant decrease in B_r was also recognized. Coene *et al.*[12] found that Fe_3B has an easy-plane anisotropy and must be soft magnetic. This finding is significant because it provides an experimental evidence for a theoretical magnet proposed by Kneller and Hawig[13]; "the exchange-spring magnet" composed of mutually exchange-coupled nanocrystalline mixture of a soft magnetic phase and a hard magnetic phase.

The present authors recently discovered that both H_{cJ} and B_r are enhanced by simultaneous addition of Co and M, where M is one of Al, Si, Cu, Ga, Ag, and Au to the ternary system[14-16]. Also revealed was that Dy, when used with these additives, increases H_{cJ} without decreasing B_r. These improvements have been attributed to pronounced refinement of grain sizes of the crystallized materials. The purposes of the present paper are to investigate the effects of the additives on the crystallization behavior of the precursor amorphous materials and to discuss the relation between the microstructure and magnetic properties of this type of permanent magnets, which may best be referred as Fe_3B-$Nd_2Fe_{14}B$ type.

2. PROCESSING PROCEDURE AND MICROSTRUCTURE DEVELOPMENT

$Nd_{4.5-x}Fe_{77-y-z}B_{18.5}Dy_xT_yM_z$, where T = V or Co and M = Si or Ga, is the formula of the magnets described in this paper (see Table 1). The Fe_3B-$Nd_2Fe_{14}B$ nanocrystalline magnets are produced from amorphous via a crystallization heat treatment. The precursor materials need not to be perfectly amorphous for the development of the very fine microstructure. Heat treatment is performed above crystallization temperatures (T_x) of Fe_3B and $Nd_2Fe_{14}B$ phases, which are shown in

Table 1.
Composition, crystallization temperatures, and magnetic properties of $Nd_{4.5-x}Fe_{77-y-z}B_{18.5}Dy_xT_yM_z$ (T = V or Co; M = Si or Ga) crystallized flakes. Density is assumed to be 7.50 Mg/m^3.

Compsition	T_x(K)[a]		H_{cJ}(MA/m)	B_r(T)	$(BH)_{max}$	J_S(T)	T_c(K)[b]		
	Fe_3B	$Nd_2Fe_{14}B$			(kJ/m^3)		T_{c1}	T_{c2}	T_{c3}
$Nd_{4.5}Fe_{77}B_{18.5}$	857	878	0.29	1.19	107	1.47	766	539	1043
$Nd_{4.5}Fe_{74}Co_3B_{18.5}$	855	877	0.34	1.20	123	1.47	776	649	1098
$Nd_{4.5}Fe_{74}V_3B_{18.5}$	876	910	0.37	0.99	90.2	1.22	753	583	1041
$Nd_{4.5}Fe_{73}Co_3Ga_1B_{18.5}$	855	871	0.34	1.21	128	1.42	779	650	1084
$Nd_{3.5}Dy_1Fe_{73}Co_3Ga_1B_{18.5}$	865	893	0.39	1.18	136	1.37	775	646	1084
$Nd_{4.5}Fe_{73}V_3Si_1B_{18.5}$	884	918	0.37	1.05	109	1.25	743	599	1039
$Nd_{4.5}Fe_{73}Co_3Si_1B_{18.5}$	868	880	0.34	1.23	134	1.45	773	641	1083

a) T_x in this table corresponds to a temperature at which an exsothermic peak sets on upon heating at 0.17 K/s in DTA.

b) T_{ci} with i = 1, 2, 3 corresponds to T_c's of Fe_3B, $Nd_2Fe_{14}B$, and bcc Fe phases, in which the additive elements partly substitute Fe, respectively.

Table 1 as determined from the onset of exsothermic peaks in differential thermal annalysis (DTA). The crystallization temperatures, especially those of the $Nd_2Fe_{14}B$ phase, are strongly dependent on the T and M elements.

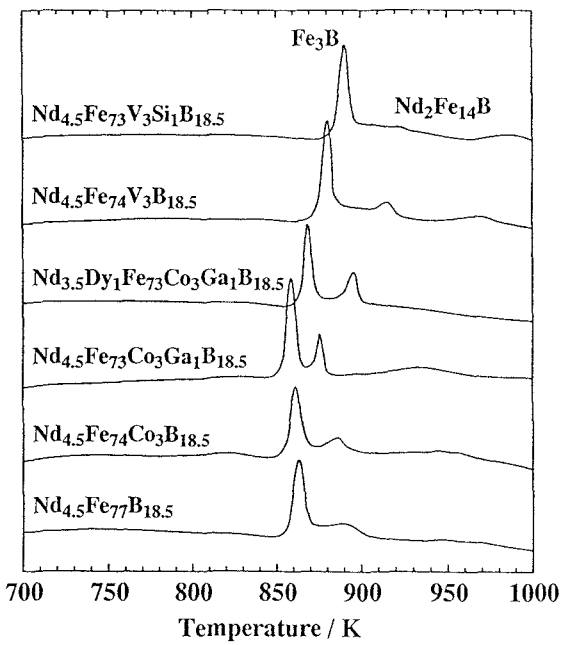

Fig. 1 DTA curves of the initially amorphous flakes upon heating at 0.17 K/s.

By the heat treatment, the nearly amorphous precursor is transformed into a nanocrystalline mixture of tetragonal (I4) Fe_3B, tetragonal ($P4_2/mnm$) $Nd_2Fe_{14}B$, and bcc Fe. V and Co are believed to replace Fe partly in these phases. The nanocrystalline structure is metastable, and heat treatment at too high a temperature destroys the structure either by coarsening the grain size or by phase transformation into the thermally equilibrium phases, bcc Fe, Fe_2B, and $Nd_{1.1}F_4B_4$. Transmission electron microscopy (TEM) has revealed that the typical grain size in the optimally heat-treated materials containing both T and M is in the 10-20 nm range, which is significantly smaller than the typical grain size of 50 nm observed in the ternary Nd-Fe-B materials of this type. The quaternary magnets Nd-Fe-T-B without the M elements have coarsened grains of a size of approximately 70nm among smaller grains of 50 nm sizes. Examples of TEM observations are shown in Fig. 2 for the case of V-Si addition. Identification of the coarser grains awaits further investigations.

3. MAGNETIC PROPERTIES

Magnetic poperties of the magnets investigated are listed in Table 1. The largest saturation magneti-

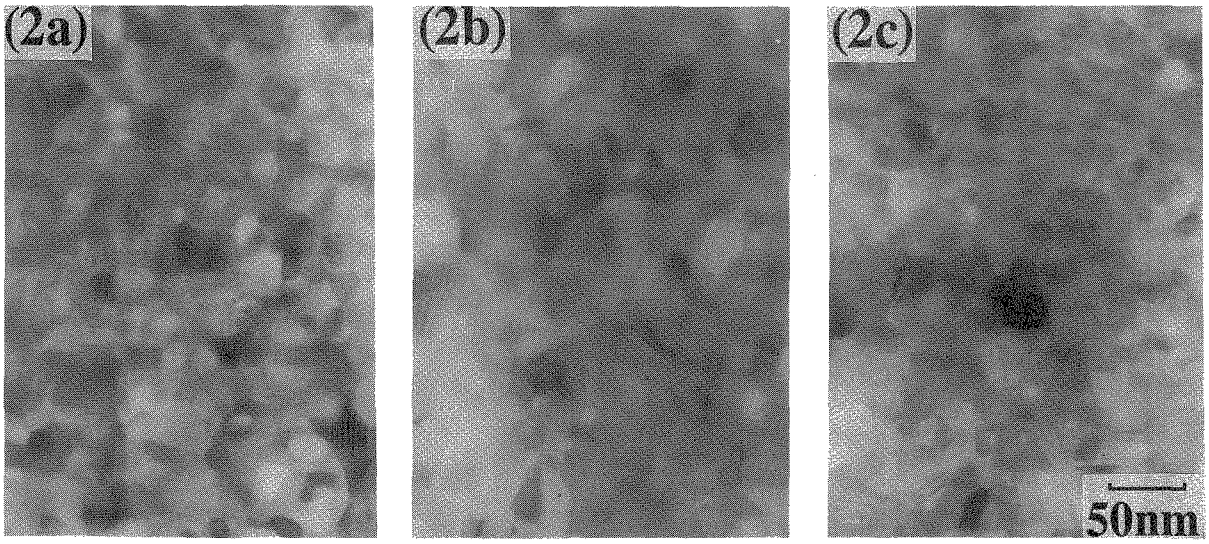

Fig. 2 TEM photographs of optimally crystallized $Nd_{4.5}Fe_{77}B_{18.5}$ (a), $Nd_{4.5}Fe_{74}V_3B_{18.5}$ (b), and $Nd_{4.5}Fe_{73}V_3Si_1B_{18.5}$(c).

zation (J_S) is observed in the ternary Nd–Fe–B system. Alloying only V or Co causes a decline in both J_S and B_r and an increase in H_{cJ}. The change in J_S is attributable to the replacement of Fe magnetic moments with smaller (or null) moments of Co (or V). The decrease in B_r is due not only to the decrease in J_S but also to a weakening of the remanence enhancement phenomenon, which may be a result of the grain coarsening. In the Nd–Fe–B–T–M system, on the other hand, a significant remanence enhancement is present, resulting in an increase in $(BH)_{max}$.

Of an importance is the increase in H_{cJ} upon alloying the T elements. The most pronounced effect has been observed in the case of the V addition. The value of H_{cJ} obtained in this study is considerably higher than H_{cJ} of 0.28 kA/m reported by Kneller and Hawig for $Nd_{3.8}Fe_{73.3}B_{18.0}V_{3.9}Si$[13].

The temperature dependence of magnetization in the Fe_3B–$Nd_2Fe_{14}B$ type magnets is primarily determined by the main phase Fe_3B. Due to the high Curie temperature of this phase, near 786 K, the temperature coefficient of B_r is in the range between −0.08 %/K and −0.05 %/K near room temperature. Coercivity vanishes at Curie temperature of the $Nd_2Fe_{14}B$ phase as already reported for the ternary case[6]. The temperature coefficient of H_{cJ} is typically −0.35 %/K.

4. MAGNETIC HARDENING MECHANISM

The Fe_3B–$Nd_2Fe_{14}B$ type magnets show a pronounced recoil behavior[13–16]. That is; once saturated by a large field in one direction, magnetization springs back even from the H_{cJ} point when the demagnetizing field is removed. Presumably, such a strong recoil behavior is a signature of the exchange–spring mechanism proposed by Kneller and Hawig[13]. The theoretical requirement for this phenomenon to occur is that the size of the soft magnetic phase is significantly smaller than the width of domain walls in the (hypothetically large) soft magnetic phase. Since the relative strength of the intergrain exchange interactions increases with decreasing the grain size, the squareness of the hysteresis curve should be improved with decreasing the grain size. Therefore, the enhanced B_r and $(BH)_{max}$ realized by alloying the T–M additives are attributable to refinement of grain sizes.

When the remanence enhancement occurs in

Table 2
Magnetic properties of compression-molded resin-bonded magnets produced from the improved Fe_3B-$Nd_2Fe_{14}B$ type magnetic materials.

Compound[a)]	Density (Mg/m^3)	B_r (T)	$(BH)_{max}$ (kJ/m^3)	H_{cJ} (kA/m)	H_M[b)] (MA/m)
1	6.0	0.86	66.1	0.31	1.14
2	5.9	0.79	64.8	0.39	2.54
3	5.7	0.71	57.3	0.40	2.11

a) 1 = $Nd_{4.5}Fe_{73}Co_3GaB_{18.5}$, 2 = $Nd_{3.5}DyFe_{73}Co_3GaB_{18.5}$, 3 = $Nd_{4.5}Fe_{73}V_3SiB_{18.5}$, all mixed with 2 wt% epoxy.
b) H_M stands for the magnetizing force required to obtain a 95% saturation of residual open magnetic flux for a permeance coefficient of one.

isotropic nanocrystalline $Nd_2Fe_{14}B$ magnets, there is a loss on the part of anisotropy energy for a gain in the exchange energy[17]. In the Fe_3B-$Nd_2Fe_{14}B$ magnets, which are isotropic, the similar mechanism may apply. However, the loss of the anisotropy should be much less than the $Nd_2Fe_{14}B$ case because of the soft magnetic nature of Fe_3B. As a result, H_{cJ} does not decrease with decreasing the grain size as does in the case of nano-crystalline isotropic $Nd_2Fe_{14}B$ type magnets.

5. RESIN-BONDED MAGNETS

The Fe_3B-$Nd_2Fe_{14}B$ type magnets with the improved coercivity may be exploited in the form of isotropic resin-bonded magnets. Table 2 shows examples of magnetic performances of such magnets produced by means of the compression-molding technique.

Temperature range in which the bonded magnets are exposed is restricted near room temperature. Therefore, the relatively small coercivity, which in turn assures easy magnetizing (or "charging") of the magnets[14-16], is not a detracting factor because the relatively good temperature coefficient of H_{cJ} of -0.35 %/K is available.

The temperature coefficient of B_r is comparable with that of Sm-Co magnets. Together with the high value of B obtainable with limited magnetizing forces, the isotropic resin-bonded magnets produced from the improved Fe_3B-$Nd_2Fe_{14}B$ type Nd-(Dy)-Fe-B-T-M magnetic materials may be most suitable for small stepping motors.

ACKNOWLEDGEMENT

The authors are indebted to Mr. Minoru Uehara for the TEM observations.

REFERENCES

1. R. Coehoorn, D. B. Mooij, J. P. W. B. Duchateau, and K. H. J. Buschow, J. Phys. (Paris) Colloq. 8 (1988) 669.
2. K. H. J. Buschow, D. B. de Mooij, and R. Coehoorn, J. Less-Common Met. 145 (1988) 601.
3. R. Coehoorn, D. B. de Mooij, and C. de Waard, J. Magn. Magn. Mater. 80 (1989) 101.
4. B.-G. Shen, J.-X. Zhang, L.-Y. Yang, F. Wo, T.-S. Ning, S.-Q.-Ji, J.-G. Zhao, H.-Q. Guo, and W.-S. Zhan, J. Magn. Magn. Mater. 89 (1990) 195.
5. B.-G. Shen, L.-Y. Yang, J.-X. Zhang, B.-X. Gu, T.-S. Tai, F. Wo, J.-G. Zhao, H.-Q. Guo, and W.-S. Zhan, Solid State Commun. 74 (1990) 893.
6. L.-Y. Yang, B.-G. Shen, J.-X. Zhang, F. Wo, T.-S. Ning, J.-G. Zhao, H.-Q. Guo, and W.-S. Zhan, J. Less-Common Met. 166 (1990) 189.
7. J.-X. Zhan, B.-G. Shen, L.-Y. Yang, and W.-S. Zhan, Phys. Stat. Sol. (a) 122 (1990) 651.
8. R. Coehoorn and C. de Waard, J. Magn. Magn. Mater. 83 (1990) 228.
9. B.-G. Shen, J.-X. Zhang, L.-Y. Yang, F. Wo, T.-S. Ning, J.-G. Zhao, H.-Q. Guo, and W.-S. Zhan, J. Less-Common Met. 167 (1991) 339.
10. B.-G. Shen, L.-Y. Yang, J.-X. Zhan, F. Wo, T.-S. Ning, J.-G. Zhao, H.-Q. Guo, and W.-S. Zhan, J. Magn. Magn. Mater. 96 (1991) 335.
11. J.-X. Zhang, B.-G. Shen, L.-Y. Yang, and W.-S. Zhan, Phys. Stat. Sol. (a) 124 (1991) 541.
12. W. Coene, F. Hakkens, R. Coehoorn, D. B. de Mooij, C. de Waard, J. Fidler, and R. Grossinger, J. Magn. Magn. Mater. 96 (1991) 189.
13. E. F. Kneller and R. Hawig, IEEE Trans. Magn. 27 (1991) 3588.
14. H. Kanekiyo and S. Hirosawa, J. Magn. Soc. Jpn. 17 (1993) 185 (text in Japanese).
15. S. Hirosawa, H. Kanekiyo, and M. Uehara, J. Appl. Phys. 73 (1993) 6488.
16. S. Hirosawa, H. Kanekiyo, and M. Uehara, IEEE Trans. Magn. (to be published).
17. H. Fukunaga and H. Inoue, Jpn. J. Appl. Phys. 31 (1992) 1347.